Real Time Measurement of Multiphase Flow Velocity using Electrical Capacitance Tomography

Sidi Mohamed Ahmed Ghaly
Electrical Engineering Department, Imam Mohammad Ibn Saud Islamic University, Saudi Arabia | Département de physique, Ecole Normale Supérieure, Mauritania
smghaly@imamu.edu.sa

Mohammad Obaidullah Khan
Electrical Engineering Department, Imam Mohammad Ibn Saud Islamic University, Saudi Arabia
OKKhan@imamu.edu.sa

Mohammed Shalaby
Electrical Engineering Department, Imam Mohammad Ibn Saud Islamic University, Saudi Arabia
myshalaby@imamu.edu.sa

Khaled A. Al-Snaie
Electrical Engineering Department, Imam Mohammad Ibn Saud Islamic University, Saudi Arabia
kalsnaie@imamu.edu.sa

Majdi Oraiqat
Electrical Engineering Department, Imam Mohammad Ibn Saud Islamic University, Saudi Arabia
mtoraiqat@imamu.edu.sa

Received: 17 June 2023 | Revised: 11 July 2023 | Accepted: 16 July 2023

 DOI: https://doi.org/10.48084/etasr.6130

ABSTRACT

Accurate and real-time measurement of fluid flow velocity is crucial in various industrial processes, especially when dealing with multiple phase fluids. Traditional flow measurement methods often struggle to accurately quantify the velocity of complex multiphase flows within pipes. This challenge necessitates the exploration of innovative techniques capable of providing reliable measurements. This paper proposes the utilization of Electrical Capacitance Tomography (ECT) as a promising approach for measuring the velocity of multiple phase fluids in pipes. The ECT technique involves the non-intrusive imaging of the electrical capacitance distribution within the pipe. By utilizing an array of electrodes placed around the pipe circumference, the capacitance distribution can be reconstructed, offering insight into the fluid flow patterns. By analyzing the temporal changes in the capacitance distribution, the velocity of different phases within the pipe can be estimated. To achieve accurate velocity measurements, an ECT system needs to account for the complexities introduced by multiphase flows. Various image reconstruction algorithms, such as linear back-projection and iterative algorithms like Gauss-Newton and Levenberg-Marquardt, are employed to reconstruct the capacitance distribution. Additionally, advanced signal processing techniques, such as cross-correlation analysis and time-difference methods, are used to extract velocity information from the reconstructed images. This paper presents an experimental investigation of measuring the velocity of multiple-phase fluids in pipes using the ECT technique. The study aims to address the challenges associated with different flow regimes, fluid properties, and pipe geometries by exploring advancements in electrode design, system calibration, and data processing techniques to enhance the accuracy and robustness of ECT-based velocity measurements.

Keywords-ECT system; flow velocity; fluid velocity; electrode; sensor; image reconstruction

I. INTRODUCTION

There are available numerous non-contact techniques to measure various parameters related to electric charges carried on solid particles, such as mass flow rate, concentration, volume loading, mean flow velocity, and other electrical and mechanical properties in gas-solid flows. One such method is based on electrostatic induction. To measure these quantities without disturbing the particles, nonintrusive probes, sensors, detectors, and transducers of different shapes are employed as the initial components of measuring systems. The method described here utilizes a probe in the form of a ring-shaped metal electrode. The flow itself generates electrostatic flow noise, which induces charge or potential (or both) on the inner surfaces of the sensing devices. The magnitude of these signals is directly proportional to the measured quantities. The output signals from the sensing devices provide valuable information about the particulate flow. The evolution and historical development of this method, along with its various aspects, over the past 50 years since its initial publication, including its metrological description and practical application in charge measurement is presented in [1].

The current methods for calculating the velocity field in multiphase flows using a twin-plane electrical capacitance system are discussed in [2]. These methods allow for the determination of the velocity profile of the multiphase flow within an industrial installation. The theoretical assumptions underlying these methods are also described. The advantages and disadvantages of the proposed flow velocity measurement methods are discussed, highlighting the ability to obtain a velocity vector with three components instead of just one component as in the classical approach. These methods are based on the concept of "best correlated pixels," where pairs of pixels with the highest cross-correlation values are selected. Unlike the classical method, this concept does not require additional assumptions regarding the direction of solids within the sensor volume, which is important in cases where solids' trajectories are three-dimensional and complex. The method can be combined with ECT and potentially with other tomographic modalities. The presented results include measurements from gas/solids flows in both vertical and horizontal channels. The authors suggest that this technique can be further applied for solids mass flow measurement, leading to the development of a more accurate solids mass flow meter and enabling the analysis of swirl flow with high accuracy in the future.

The application of cross correlation signal processing in engineering is discussed in [3], particularly for velocity measurements in challenging fluid environments. The importance of accurate velocity evaluation is emphasized and the study is divided into two parts: practical execution and data acquisition analysis. Various techniques and multiphase flow sensors are used for velocity evaluation, such as ultrasonic sensors, capacitive sensors, and electrostatic sensors. The comparative study focuses on using ring-shaped electrostatic sensors to determine the velocity of gas/solid two-phase flow in a coal test-rig at Teesside University. The data acquired from the test-rig are processed with LabVIEW software. The paper presents the results and outputs of cross correlation velocity measurement, providing a step-by-step explanation of the gas/solid two-phase flow process, including pneumatic conveying, the flow process of "fillite" particles, electrostatic sensing mechanism, and velocity measurement. Additionally, it highlights the improvement in accuracy achieved through software-based analysis in the data acquisition process using LabVIEW virtual instruments.

In [4], ultrasonic transmission mode tomography is utilized to visualize the flow of a two-phase liquid/gas mixture in a pipe or vessel. The sensing element comprises ultrasonic transceivers, specifically 8, 16, and 32 units, strategically placed to cover different sections of the pipe over time. The objective of this study is to determine the optimal number of transceivers that yield the best performance and provide a clear image of the liquid/gas flow. The paper describes the development of the system, including the ultrasonic transduction circuits, electronic measurement circuits, data acquisition system, and image reconstruction techniques. Ten different liquid-gas flow conditions were simulated, and the system successfully visualized the internal characteristics and generated concentration profiles for both the liquid and gas phases. Among the tested configurations, the system using 32 transceivers produced the highest-quality images for all 10 flow conditions. Transceivers offer a cost-effective and non-invasive method for ultrasonic tomography, requiring a low operating voltage as long as the acoustic energy can pass through the vessel. Increasing the number of transceivers helps improve measurement resolution, reduce spatial image errors, and enhance measurement accuracy. However, using 32 transceivers slows down the system due to the extended processing time required for data analysis from these transceivers.

In [5], an electrostatic, non-contact technique was presented that builds upon a previously developed method for continuously measuring electric charges carried by solid particles in two-phase particulate flow within pneumatic transport pipelines. The authors present a measuring system based on a microcomputer and share some preliminary test results. This system enables continuous and noncontact measurements of both the average velocity of the flow and the mass flow rate.

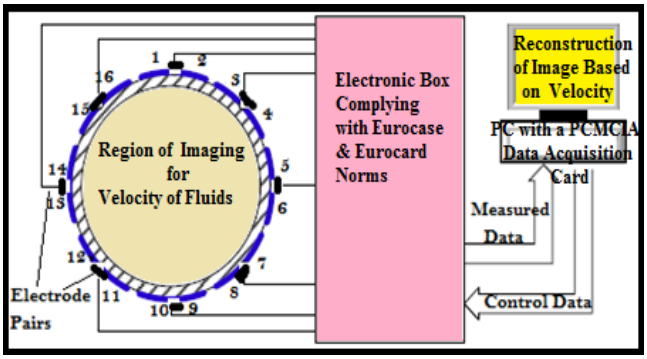

Fig. 1. Typical block diagram of the ECT-based velocity sensor.

The proposed technique has wide-ranging applications in various industries, including petroleum, chemical, and food

processing. It can provide valuable insight into the flow behavior of complex multiphase fluids, aiding process optimization, troubleshooting, and quality control. Additionally, the non-invasive nature of ECT makes it a favorable choice for monitoring flow dynamics without disturbing the system integrity. A typical block diagram of the ECT-based velocity measurement system is shown in Figure 1.

II. ELECTRICAL MODELING

A typical approach to accurately measure the flow velocity in non-uniform single-phase flows is discussed in [3]. Authors in [4] describe multiphase flow measurements which are relatively deviating from the profile of ECT velocity. However, these types of flow meters do not supply information on the local axial velocity distribution in the flow cross-section. This may be a big lacuna, particularly in a steady multiphase flow where, for instance, the parameter flow rate Qc can only be calculated from the steady local velocity V_C and the parameter steady fraction α_C, of the phase in the flow cross section A as illustrated in (1) [6]:

$$Q_C = \int_A V_C \alpha_C \, dA \tag{1}$$

The fundamental concept of electromagnetic flow meters (EMFMs) illustrates that charged particles, in a conducting material which moves under a magnetic field, experience or exert a Lorentz force acting in the direction perpendicular to both the material's motion and the applied magnetic field. For a uniform velocity profile the flow rate is directly proportional to the voltage measured between the two electrodes [7]. The local current density j in the fluid obeys Ohm's law in the form of:

$$j = \sigma(E + VxB) \tag{2}$$

where σ represents the local fluid conductivity, V represents the local fluid velocity, B represents the local magnetic flux density, and E represents the electric field due to charges distributed in and around the fluid. The product term (VxB) represents the local electric field induced by the fluid motion. For certain fluids in which the conductivity variations are relatively minor, such as the single phase and the multiphase flows, (2) was simplified [8] to demonstrate that the local potential U in the flow can be obtained by solving:

$$\nabla^2 U = \nabla \cdot (v \times B) \tag{3}$$

Considering a circular cross section flow channel (glass pipe) bounded by a number of electrodes, with a uniform magnetic field of flux density $\bar{B}$ normal to the axial flow direction, it can be shown according to [8] that in a steady flow, the potential difference U_j between the j^{th} pair of electrodes can be given by:

$$U_j = \frac{2\bar{B}}{\pi a} \iint v(x,y) W(x,y) dx \, dy \tag{4}$$

where $v(x, y)$ represents the steady local axial flow velocity at the coordinates (x, y) in the flow cross-section, $W(x,y)$ represents a parameter called weight value relating the contribution of $v(x, y)$ to U_j and a represents the internal radius of the flow channel (glass pipe). Equation (4) can be discredited as follows by an assumption that the flow cross section can be divided into $\hat{I}$ elemental regions:

$$U_j = \frac{2\bar{B}}{\pi a} \sum_{n=1}^{j} \hat{v}_n \hat{W}_{nj} \hat{A}_n \tag{5}$$

where $\hat{v}_n$ represents the local axial velocity in the nth elemental region and $\hat{A}_n$ represents the cross-sectional area of the n^{th} elemental region. The variable $\hat{W}_{nj}$ represents the weight value with the contribution of the axial velocity in the n^{th} elemental region to the j^{th} potential difference U_j. At the instance, assuming the axial flow velocity to be constant in each of N large regions, (5) can be modified as:

$$U_j = \frac{2\bar{B}}{\pi a} \sum_{n=1}^{N} \hat{V}_i \sum_{n=\hat{\imath}_{-1}+1}^{\hat{\imath}_i} \hat{w}_{nj} \hat{A}_n \tag{6}$$

where $\hat{V}_i$ represents the axial flow velocity in the i^{th} large region. In the above relation, when the subscript n is in the range of $\hat{\imath}_{-1} + 1 \leq N \leq \hat{\imath}_i$, it refers to the elemental regions lying within the i^{th} large region (it can also be noted that there are $\hat{\imath}_i$ to $\hat{\imath}_{i-1}$ elemental regions within the i^{th} large region). An "area weighted" mean weight value w_{ij} related to the contribution of the velocity $\hat{V}$ in the i^{th} large region to the j^{th} potential difference U_j is given by:

$$w_{ij} = \frac{\sum_{n=i_{i-1}+1}^{i_i} \hat{w}_{n_i} \hat{A}_n}{A_i} \tag{7}$$

where A_i represents the cross-sectional area of the i^{th} large region. Combining (6) and (7) yields:

$$U_j = \frac{2\bar{B}}{\pi a} \sum_{i=1}^{N} v_i w_{ij} A_i \tag{8}$$

It can be seen that the reciprocal of (8) enables computing the estimates of the local axial flow velocity in each of the N large pixels to be determined from N potential difference measurements U_j made on the boundary of the flow. Nevertheless, (8) was derived based on the assumption that the axial velocity in each large pixel is constant, it will be seen that when this inversion method is used to solve for the velocity in each large pixel, then the obtained values of v_i give a good approximation to the mean axial velocity in each of the large pixels, in situations where there is some axial velocity variation within each large pixel [7-8].

III. EXPERIMENTAL SETUP

To carry out the experiment, a test rig was set up with a see-through pipe section to facilitate visual observations. The ECT system consisted of an array of N electrodes fixed around the pipe circumference separated with equal distances. A controlled flow of multiple phase fluids, such as gas-liquid or liquid-liquid mixtures, can be introduced into the pipe, covering a range of flow rates and compositions. The electrode design is optimized to minimize signal interference and to maximize sensitivity for changes in the capacitance distribution. The system calibration procedures are first performed to avail accuracy in the measurement and then this system was used to measure the fluid flow velocity [9]. Data acquisition is carried out continuously by measuring the capacitance values at each electrode position throughout the experiment. The obtained data are then processed using digital signal processing techniques, including cross-correlation analysis and time-difference methods, to extract the velocity information from the reconstructed capacitance distribution.

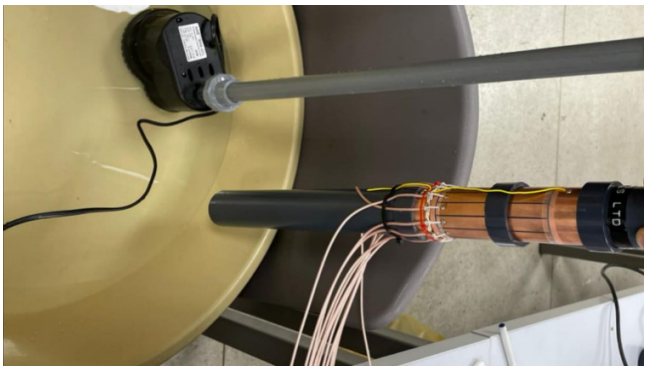

Fig. 2. Typical test rig setup with ECT N-electrode sensor.

A typical example of experiment results for the determination of oil velocity through a pipe using ECT is demonstrated in Figure 2. In the experimental setup, a typical test rig arrangement is availed in which a pipe with a diameter of 11 cm with a suitable length is used. The pipe circumference ECT sensor array has 16-to-8 customized electrodes fixed evenly as illustrated in Figure 3. This sensor has the following dimensions: Electrode = 15 cm ×1.96 cm, gap between the electrodes = 0.2 cm, external circumference of the pipe = 34.5 cm, outer radius of the pipe = 5.5 cm, inner pipe cross section area = 95 cm^2, total volume of the ECT section (electrode region) V_{total} = 95 × 15 = 1425 cm^3. The customized 16-8 electrode ECT sensor behaves the same as that of a 16-electrode ECT sensor operating as 8 electrodes rotating 1 electrode to the left and 1 to the right by employing relays as illustrated in Figure 3. The purpose of this configuration is to improve the sensitivity and the accuracy of the reconstructed images. To facilitate this, 8 relays are electrically coupled such that the common of each relay is connected to the odd electrode (1, 3, 5,…, 15) and the adjacent electrode in the clockwise direction is connected to the normally open pin of this relay, whereas the adjacent electrodes in the counter-clockwise direction are connected to the normally closed pin of the same relay [10-11]. The fluid in the pipe (oil-water or mixtures of different fluids and gas) is allowed to flow with a flow rate of 1-5 lt/s in steps of 0.5 lt/s. A calibration process is performed with different oil flow rates, and the corresponding capacitance changes are recorded.

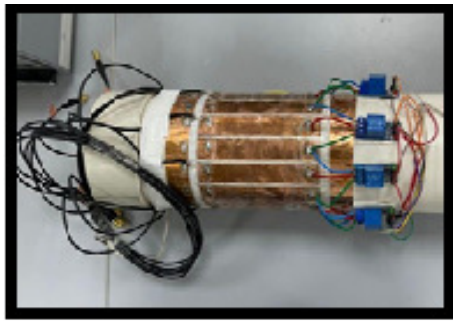

Fig. 3. The customized 16-to-8 electrode ECT sensor.

For data acquisition and image reconstruction, an ACECT system is employed which uses an AC-based capacitance measuring circuitry with a high-frequency sinusoidal excitation signal generator and a Phase-Sensitive Demodulator (PSD). This circuit can detect and record the change in capacitance with 0.0001 pF precision at considerably high speed. This system can receive image data at 140 fps from a typical *N*-electrode sensor. Because of the inbuilt DDS signal generators employed inside, the excitation frequency can be programmed, resulting in spectroscopic measurements. Further, the hardware design allows any electrode combination topologies to be used, offering high flexibility in setting up different excitation patterns. The ACECT system broadly comprised of three prime parts:

- An electronics box complying in accordance with the Eurocase and Eurocard norms, which can hold up to 16 measuring channels;
- A PC with a PCI data acquisition board / a laptop PC with a PCMCIA data acquisition card and
- An *N*-electrode demonstration sensor section.

The oil flow is initiated through the pipe, and the ECT system captures the capacitance measurements over the time of flow. The acquired capacitance data are processed and reconstructed into an image representing the oil distribution within the pipe. This paper highlights the potential of ECT as an effective technique for measuring the velocity of multiple phase fluids in pipes. It identifies future research directions to further improve the accuracy, reliability, and applicability of ECT-based flow velocity measurements in diverse industrial settings.

IV. IMPLEMENTATIN FOR VELOCITY MEASUREMENT

From the capacitance measurements, the oil velocity can be determined based on the calibration data. Typically, a subset of adjacent electrode pairs is chosen to monitor the fluid flow and calculate the velocity. The capacitance changes between these selected electrode pairs are then correlated with the fluid velocity using calibration data or mathematical models. This approach allows for efficient measurement and analysis of velocity without the need to measure the capacitance between all the electrodes. The selection of electrode pairs for velocity measurement depends on the specific application and the desired sensitivity to velocity changes in certain regions of the pipe. By strategically choosing electrode pairs and analyzing the corresponding capacitance changes, one can accurately determine the fluid velocity within the pipe. For example, if there is a particular area where velocity changes are expected to be significant or if there is a known flow disturbance, electrode pairs can be strategically positioned in that region to capture the velocity variations accurately.

To study the effect of the number of electrodes on the sensitivity of detecting fluid velocity in the container pipe at a relatively high speed compared to the speed of data acquisition, the setup was: the frequency of the excitation is 180 kHz and the time for one period of measurement is 23 ms. It is assumed that during this period of time the flow doesn't move by more than one tenth of the electrode length which is 1.5 cm. Therefore, the maximum speed of the flow is given by:

$\frac{1.5\ cm \times 10^{-2}}{23\ ms \times 10^{-3}}$ = 0.625 m/s equal to 6.194 lt/s

For the flow measurement of the fluid by the customized 16-8 electrode sensor, the sensor is calibrated with the full state as water and the empty state as air. The water is chosen as a fluid and measurements were performed with the said specifications. The obtained images are illustrated in Figure 4. The water is allowed to flow from the axial center of the hollow pipe surrounded by air inside both the said ECT sensors. It is evident and can be clearly seen from these images that, for the same flow speed, image clarity is better for the customized 16-8 electrode ECT sensor and the random occurrence of air bubbles at different instants with different oil flow velocities [12-13].

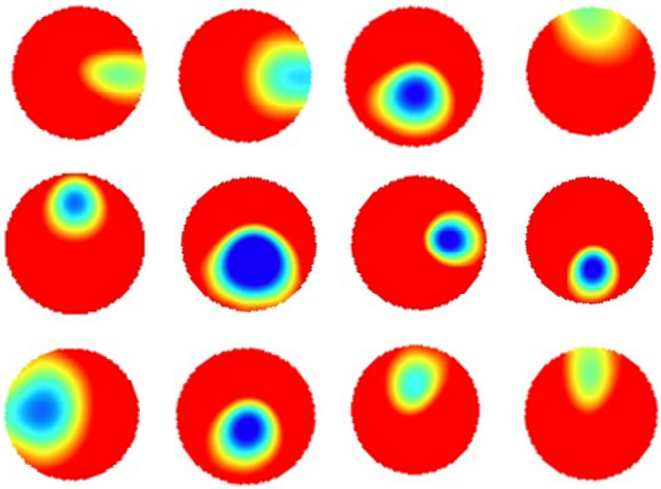

Fig. 4. Random occurrence of air bubbles at different instants with different oil flow velocities.

Figure 5 illustrates the variation of oil flow velocity at different parts of the pipe cross section showing its turbulence nature. The overall flow velocity is controlled to be at 2 lt/s.

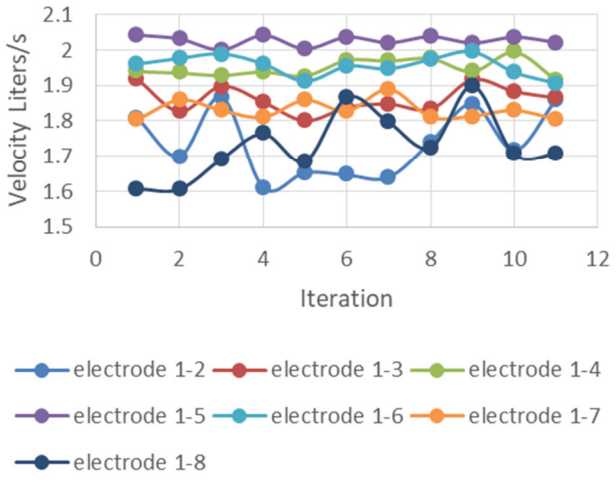

Fig. 5. The variation of oil flow velocity at different parts of the pipe cross section showing its turbulence nature.

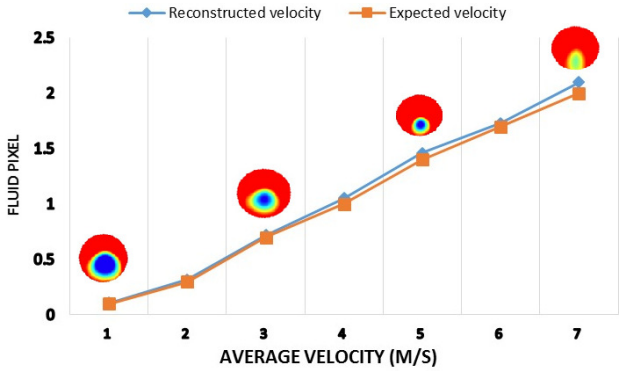

Fig. 6. Convertion of velocity into image pixel profiles.

The velocity of the liquid inside the sensor induces a voltage that can be measured. This can be converted into pixel gray level or intensity of the pixel component of the image obtained [14]. In the case of the 8-16 ECT sensor, 7 independent potential difference measurements were performed. Also, it should be noted that the accuracy of the velocity reconstruction model depends on the number of electrodes used in the ECT sensor. The measurement results that convert velocity into image pixel profile are shown in Figure 6. Thus, a real-time measurement of the reconstructed velocity profiles in terms of the original expected velocity profiles was carried out for 8-16 electrode ECT sensor.

V. DISCUSSION

This work is an extension of a series of articles published/accepted by the authors. In this paper, a typical customized 16-8 electrode ECT sensor is proposed and implemented experimentally in contrast with sets of standard 8, 12, and 16-electrode ECT sensors. The results of these types of sensors are noted and compared. It is observed from the results obtained during this experiment, that the performance of the customized 16-8 electrode ECT sensor is comparatively better, and exhibits better quality and performance with respect to image and velocity reconstruction. The result comparison further demonstrated that the correlation coefficient changes from 0.61 to 0.96, and the error images is within 0.3 to 0.1 for SNRs from 60 to 90 dB. It was also observed that the reconstructed velocity profiles are consistent with the original expected velocity profiles for the customized 8-16 electrode ECT sensor [6, 15].

Furthermore, the images are represented as direct functions of the imposed mean flow velocity. Each pixel of the image reflects the flow velocity of the liquid, which is actually extracted from the voltage difference measurement matrix. Closely inspecting Figure 6, it can be seen that the reconstructed velocity profiles are consistent with the original imposed velocity profiles for the custom 8-16 electrode ECT sensor.

VI. CONCLUSION

The experimental results revealed promising capabilities of the ECT technique in accurately measuring the velocity of multiple phase fluids in closed containers or pipes. The reconstructed capacitance distribution provided valuable

insight into the flow patterns and dynamics, allowing for the estimation of flow velocities. The findings of this experimental study contribute to the understanding and application of ECT in multiphase flow measurements. The identified advancements in electrode design, system calibration, and data processing techniques offer practical solutions for improving the accuracy and robustness of ECT-based velocity measurements in real-world industrial scenarios.

This experimental investigation demonstrates the potential of ECT as a reliable technique for measuring the velocity of multiple phase fluids in pipes. The obtained results pave the way for further research and development, focusing on optimizing the ECT system parameters and expanding its applicability across various industrial sectors where accurate flow velocity measurements are essential.

ACKNOWLEDGMENT

This project was funded by the National Plan for Sciences, Technology and Innovation (MAARIFAH) – King Abdulaziz City for Science and Technology – The Kingdom of Saudi Arabia, award number (14-ELE741-08).

REFERENCES

[1] J. B. Gajewski, "Electrostatic Nonintrusive Method for Measuring the Electric Charge, Mass Flow Rate, and Velocity of Particulates in the Two-Phase Gas–Solid Pipe Flows—Its Only or as Many as 50 Years of Historical Evolution," *IEEE Transactions on Industry Applications*, vol. 44, no. 5, pp. 1418–1430, Sep. 2008, https://doi.org/10.1109/TIA.2008.2002276.

[2] V. Mosorov, K. Grudzień, and D. Sankowski, "Flow Velocity Measurement Methods Using Electrical Capacitance Tomography," *Informatyka, Automatyka, Pomiary w Gospodarce i Ochronie Środowiska*, vol. 7, no. 1, pp. 30–36, Mar. 2017, https://doi.org/10.5604/01.3001.0010.4578.

[3] M. W. Munir and B. A. Khalil, "Cross Correlation Velocity Measurement of Multiphase Flow," *International Journal of Science and Research*, vol. 4, no. 2, pp. 802–807, 2013.

[4] Z. Zakaria, M. H. F. Rahiman, and R. A. Rahim, "Simulation of the Two-Phase Liquid - Gas Flow through Ultrasonic Transceivers Application in Ultrasonic Tomography - ProQuest," *Sensors & Transducers*, vol. 112, no. 1, pp. 24–38, Jan. 2010.

[5] J. B. Gajewski, B. J. Glod, and W. S. Kala, "Electrostatic method for measuring the two-phase pipe flow parameters," *IEEE Transactions on Industry Applications*, vol. 29, no. 3, pp. 650–655, Feb. 1993, https://doi.org/10.1109/28.222440.

[6] S. M. A. Ghaly, K. A. Al-Snaie, M. O. Khan, M. Y. Shalaby, and M. T. Oraiqat, "Design and Simulation of an 8-Lead Electrical Capacitance Tomographic System for Flow Imaging," *Engineering, Technology & Applied Science Research*, vol. 11, no. 4, pp. 7430–7435, Aug. 2021, https://doi.org/10.48084/etasr.4122.

[7] S. M. A. Ghaly *et al.*, "Diagnosis of Two-Phase Oil/Gas Flow in a Closed Pipe using an 8-Electrode ECT System," *Engineering, Technology & Applied Science Research*, vol. 13, no. 4, pp. 11332–11337, Aug. 2023, https://doi.org/10.48084/etasr.6011.

[8] S. M. A. Ghaly *et al.*, "A 12-Electrode ECT Sensor with Radial Screen for Fluid Diagnosis," *Engineering, Technology & Applied Science Research*, vol. 13, no. 4, pp. 11393–11399, Aug. 2023, https://doi.org/10.48084/etasr.6030.

[9] F. Alorifi, S. M. A. Ghaly, M. Y. Shalaby, M. A. Ali, and M. O. Khan, "Analysis and Detection of a Target Gas System Based on TDLAS & LabVIEW," *Engineering, Technology & Applied Science Research*, vol. 9, no. 3, pp. 4196–4199, Jun. 2019, https://doi.org/10.48084/etasr.2736.

[10] S. M. A. Ghaly, "LabVIEW Based Implementation of Resistive Temperature Detector Linearization Techniques," *Engineering, Technology & Applied Science Research*, vol. 9, no. 4, pp. 4530–4533, Aug. 2019, https://doi.org/10.48084/etasr.2894.

[11] R. K. Rasel, B. J. Straiton, Q. M. Marashdeh, and F. L. Teixeira, "Flow Loop Study of ECT-Based Volume Fraction Monitoring in Oil–Water Two-Phase Flows," *IEEE Transactions on Instrumentation and Measurement*, vol. 71, pp. 1–6, 2022, https://doi.org/10.1109/TIM.2022.3181929.

[12] L. Li, P. Zhang, X. Lei, and G. Xu, "Design of Array Electrode Sensor for Buried Oil Tank ECT System," in *2021 3rd International Conference on Intelligent Control, Measurement and Signal Processing and Intelligent Oil Field (ICMSP)*, Xi'an, China, Jul. 2021, pp. 22–25, https://doi.org/10.1109/ICMSP53480.2021.9513407.

[13] Z. Li, S. Xiao, Q. Yue, and T. Wang, "Electrical Capacitance Tomography Sensor With House Structure for Assisting Recognition of Objects," *IEEE Sensors Journal*, vol. 22, no. 5, pp. 4534–4544, Mar. 2022, https://doi.org/10.1109/JSEN.2022.3143709.

[14] S. M. Chowdhury, I. Nayak, Q. M. Marashdeh, and F. L. Teixeira, "Developments on Imaging and Velocimetry of Dynamic Two-Phase Flows with Electrical Capacitance Tomography Sensors," in *2022 IEEE International Symposium on Antennas and Propagation and USNC-URSI Radio Science Meeting (AP-S/URSI)*, Denver, CO, USA, Jul. 2022, pp. 1708–1709, https://doi.org/10.1109/AP-S/USNC-URSI47032.2022.9886753.

[15] S. M. A. Ghaly, M. O. Khan, M. Y. Shalaby, K. A. Al-snaie, and M. Oraiqat, "Image and Velocity profile reconstruction using a Customized 8-16 Electrode Electrical Capacitance Tomography Sensor Based on LabVIEW Simulation," *Journal of Nanoelectronics and Optoelectronics*, accepted in June 2023.